Article

Bifunctional Application of Viologen-MoS₂-CNT/Polythiophene Device as Electrochromic Diode and Half-Wave Rectifier

Suchita Kandpal, Tanushree Ghosh, Chanchal Rani, Manushree Tanwar, Meenu Sharma, Sonam Rani, Devesh K. Pathak, Ravi Bhatia, I. Sameera, Jesumony Jayabalan, and Rajesh Kumar*

Cite This: *ACS Mater. Au* 2022, 2, 293–300

Read Online

| ACCESS | Metrics & More | Article Recommendations | Supporting Information |

ABSTRACT: A dual purpose solid state electrochromic diode has been fabricated using polythiophene (P3HT) and ethyl Viologen (EV), predoped with multiwalled carbon nanotubes (MWCNTs) and MoS₂. The device has been designed by considering two important aspects, first, the complementary redox activity of P3HT and EV and second, the electron holding properties of MoS₂ and MWCNTs. The latter is found to enhance the electrochromic performance of the solid state device. On the other hand, the complementary redox nature gives the asymmetric diodic I–V characteristic to the device which has been exploited to use the electrochromic device for rectification application. The MoS₂ nanoflower and MWCNTs are synthesized by one-step hydrothermal and pyrolysis techniques and well characterized by scanning electron microscopy (SEM), X-ray analysis (XRD), and Raman spectroscopy. Electrochromic properties of the device have been studied in detail to reveal an improvement in device performance in terms of faster speed and high coloration efficiency and color contrast. In situ bias-dependent Raman spectroscopy has been performed to understand the operation mechanism of the electrochromic diode which reveals (bi-)polaron formation as a result of dynamic doping eventually leading to color change. A half-wave rectifier has been realized from the electrochromic diode which rectifies an AC voltage of frequency 1 Hz or less making it suitable for low frequency operation. The study opens a new possibility to design and fabricate multipurpose frequency selective electrochromic rectifiers.

KEYWORDS: *Electrochromic diode, P3HT, MoS₂, MWCNTs, Viologen, organic rectifiers*
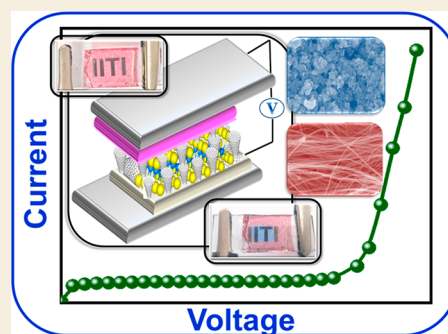
1. INTRODUCTION

Electrochromism[1,2] is a phenomenon, shown by some material (known as electrochromic materials), of an electrical bias induced change in optical properties as can be seen through the naked eye and/or in terms of modulation in absorption or transmission spectrum. An electrochromic device (ECD), fabricated utilizing the electrochromic properties of any material, is mainly used for applications in electronic curtains, smart windows, color filters including heat shielding, and so forth.[3−7] However, recently such devices have gotten a lot of interest due to additional applications in various fields like storage devices,[8−11] sensors,[12−14] special displays,[15−18] and other electronic circuits.[19] A typical ECD comprises thin films of electrochromic materials, ion transport material (electrolyte), and sometimes counterions that help to enhance the performance of the device. The color modulation in an ECD is achieved through bias-driven redox activity in materials that not only have the capabilities to exhibit two distinct redox states, but the two states should also have appreciably different optical properties. The redox reactions must occur between the electrodes to ensure a functioning ECD. For a typical ECD, the electrochromic material is the main component, which changes its color under the external bias.[20,21] Various types of materials and device paradigms, like organic,[22] inorganic (metal oxides),[23−26]

hybrid, herbal,[27] and organometallic,[28] exist that provide a variety of options for designing an application specific ECD.[29−32] However, various ways to improve electrochromic performance, preferably by using counterions and doping electrochromic layers, have been studied; multifunctional application especially as an electronic component has been explored very little.

Well-studied materials used for making ECDs include conducting polymers like polythiophene (P3HT),[20] polypyr-role, polyaniline,[33,34] Prussian blue,[12] and viologen.[35,36] Ethyl viologen (EV) and P3HT are very often used in combination due to their complementary redox behavior. Other than conducting polymers, the combination of organic and inorganic materials can also be used in EC devices, which switch in various colors because of the other ligands attached in the metal complexes. High specific surface area and unique 2D structure of the MoS₂ layers comprising S−Mo−S trilayers and coupled by

weak van der Waals force allow facile and effective insertion of charges at the interface between the film and the electrolyte, hence promoting a higher electron transfer rate, which is crucial for increasing the electrochromic properties of the device over the undoped one. Therefore, to achieve the enhanced charge transport using 2D materials like molybdenum disulfide (MoS_2) nanosheets and graphene sheets, MWCNTs as a dopant[37−39] may prove to be a good choice. Insertion of a charge carrying layer between EC conducting polymers behaves like a rectifying diode[40] with coloration occurring in the negative (reversed) bias condition. Additionally, the complementary redox activity of EV and P3HT makes these devices asymmetric leading to observation of a diodic I−V characteristic that may be used for rectification application. This will lead to multifunctional application from these typical ECDs and will enable their use in electronics.

The aim of this paper is to fabricate a solid state electrochromic diode device and demonstrate its multifunctional properties as an electrochromic device as well as a rectifier in a single solid state device, which can be use in a rectifying the circuit to rectify lower frequency of sinusoidal signals. In the device, P3HT and EV layers have been deposited appropriately with the latter having a doping of MoS_2 and MWCNTs (prepared and duly characterized) for enhancing electrochromic properties. The device exhibits color switching between two colors (magenta/blue) under an electrical bias of ±1.4 V mainly due to redox induced optical modulation which is driven by dynamic doping. In situ bias dependent optical absorption spectroscopy and Raman spectroscopies have been carried out to understand the electrochromic properties and the underlying operation mechanism[41] in terms of superior redox response and coloration efficiency with a very small external bias (1.4 V). Demonstration reveals that bias-dependent UV−vis spectroscopy and electrochemical studies show a fast color switching between magenta and blue states with coloration and bleaching times of 0.47 and 0.8 s, respectively. The switching time is defined as the time taken for 90% color modulation. The device displays an overall improved performance with coloration efficiency of 642 cm^2/C, color contrast (CC) of 46%. The asymmetric nonlinear I−V characteristic was observed from the finished device to be exploited for application as a rectifier which works well for AC voltages of frequencies of 1 Hz or less. For higher-frequency AC signals the device provides a conducting path, and the rectifying nature ceases. It is important here to mention that the present paper deals with the improved electrochromic performance of a device prepared by incorporating MWCNT + MoS_2, which not only shows a fast switching of less than half a second but also can be used for rectification. It makes the prepared device usable for dual application. Additionally, doping of charge facilitating MWCNTs and MoS_2 improves the overall electrochromic performance of P3HT-EV based solid state electrochromic device which can be used for rectification purposes to filter a sinusoidal frequency signal up to 1 Hz or less. The multifunctional nature of a prepared P3HT-EV-based all-organic diode as a solid state liquid electrolyte-less electrochromic device and rectifier has been successfully demonstrated, paving the way for application of electrochromic devices in electronics.

2. EXPERIMENTAL DETAILS

2.1. Chemicals Used

Commercial grade chemicals, poly(ethylene oxide) (PEO, Alfa Aesar, MW = 100,000), ethyl viologen diperchlorate (EV, 98%, Sigma-Aldrich), poly(3-hexyl thiophene-2,5 diyl) (P3HT, regioregular, Sigma-Aldrich), 1,2-dichlorobenzene (DCB, anhydrous, 99%, Sigma-Aldrich), and acetonitrile (ACN, anhydrous, 99%, Sigma-Aldrich) were used for device fabrication in the present study.

2.2. MoS₂ and CNT Synthesis

The MoS_2 nanoflowers and MWCNTs (conductivity = 6 S/cm) used in the device have been synthesized by a facile one-step hydrothermal route[42−44] and ferrocene−toluene pyrolysis, respectively, using the recipe discussed earlier.[45,46] In a typical synthesis of MoS_2 nanoflower, 1.7 g of ammonium heptamolybedate tetrahydrate $[(NH_4)_6Mo_7O_{24}\cdot 4H_2O]$ and 3 g of thiourea (CH_4N_2S) were dissolved in 60 mL deionized water by continuous stirring for 30 min. A homogeneous colorless solution was obtained, which was transferred into a 100 mL Teflon-lined stainless steel autoclave. The autoclave was heated to 220 °C in an oven for a period of 24 h and then cooled to room temperature. The MoS_2 nanoflower sample, in the form of a black colored product, was collected after centrifugation, and was washed with deionized water and ethanol several times. At the end, the reaction product was dried using a freeze−dryer at −80 °C in vacuum.

2.3. Device Fabrication

For fabrication of the device (electrochromic diode), 0.3 wt % P3HT solution in DCB, 5 wt % PEO in ACN, and 4 wt % EV solution in ACN were prepared by using vortex mixing. The P3HT film (~1 μm thick), having conductivity of ~10^{-4} S/cm^2, was spin coated on an ITO coated glass substrate at 500 rpm for 120 s and annealed at 80 °C for 1 h, whereas a layer of EV (premixed mixed with MWCNTs/MoS_2) in a PEO matrix was obtained by a drop-casting method on another ITO coated glass substrate, and then both were assembled together with the help of double-sided tape using a simple flip-chip method. A NOVA Nanosem 450 field emission scanning electron microscope (SEM) and X-ray diffractometer (XRD) equipped with Cu K_α (Rigaku Miniflex-II) and Raman spectroscopy measurement were carried out using Horiba-JobinYovn LABRAM HR spectrometer with a 785 nm excitation source was employed for structural characterization. Electrochemical measurements have been done using a Keithley-2450 workstation.

3. RESULTS AND DISCUSSION

Prior to making devices, the synthesized MWCNTs and MoS_2 nanoflowers have been characterized by scanning electron microscopy (SEM), Raman spectroscopy, and X-ray diffraction (XRD) to know the structural and morphological information (Figure 1). The SEM micrograph (Figure 1a) displays the several-microns-long and 50−100-nm-thick tubes which can also been seen in a magnified view (inset, Figure 1a). The structural phase of the MWCNTs has been confirmed using an XRD pattern (Figure 1b) which shows the most intense peak at ~26.2° corresponding to C (002) planes, a signature of highly graphitic nature. Other XRD peaks (Figure 1b) arise from the catalytic particles present in the MWCNT sample (e.g., Fe$_3$C and α-Fe). The observed structural characteristic has been further confirmed using Raman spectroscopy (Figure 1c) that shows the three main characteristic D (1328 cm^{-1}, symmetric), G (1570 cm^{-1}, asymmetric due to D′ hump at 1612 cm^{-1}), and 2D (2650 cm^{-1}, symmetric) bands confirming the formation of good-quality MWCNTs[45,46] to be used in the electrochromic device. The SEM micrograph from synthesized MoS_2 (Figure 1d) shows a nanoflower morphology with petals oriented in random directions and thickness varying between 15 and 30 nm with nanoflower dimensions on the order of approximately a micrometer. Further XRD (Figure 1e) patterning also shows the
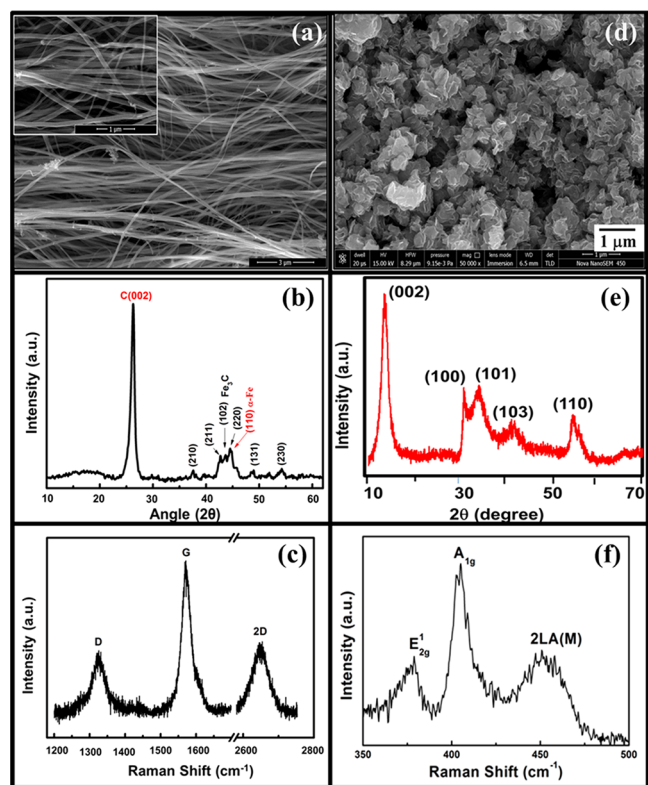
Figure 1. Basic characterizations of MWCNTs using (a) SEM, (b) XRD, (c) Raman spectroscopy, and (d−f) SEM, XRD, and Raman data, respectively, for MoS₂. Reprinted from ref 38 with the permission of AIP Publishing (copyright 2021) and ref 44 (copyright 2022).

most intense peak around ∼14° which represents a (002) plane belonging to 2H-MoS₂. All other peaks in the XRD profile also were in good agreement with the 2H-phase of MoS₂ (indexed using JCPDS card no. 37-1492). The Raman spectrum of the nanoflowers (Figure 1f) also confirms the multilayer nature of the MoS₂ petals, which is in agreement with SEM (Figure 1d). The Raman spectrum shows in-plane (E^1_{2g}) and out-of-plane (A_{1g}) vibrational modes of hexagonal MoS₂ centered at ∼379 and ∼405 cm⁻¹, respectively. The difference in the vibrational shifts of these modes is sensitive to the number of layers of MoS₂[42,43] and the value in this case is ∼26 cm⁻¹, indicating the multilayer form of MoS₂ petals. Another vibrational mode

centered at ∼451 cm⁻¹ corresponds to second-order Raman mode 2LA(M) has also been noticed.[47]

A device has been fabricated, using the formulation mentioned in the Experimental Details, which contains two layers on two ITO coated glass electrodes, which are complementary to each other. One of the ITO electrodes is coated with P3HT, an EC material, and the other one is coated with MWCNT-MoS₂ mixture doped ethyl viologen (EV). Before making the device, these two electrodes are characterized by atomic force microscopy (AFM) and scanning electron microscopy (SEM) techniques, as shown in Figure S1 in the Supporting Information (SI). The two electrodes are connected by ion-conducting PEO gel-type electrolyte as shown in the schematic (Figure 2a), which provides the path for ions to move from one electrode to another electrode under the application of external bias. The fabricated device shows an asymmetric I−V curve exhibiting diodic nature (Figure 2b) when measured in two-terminal geometry with connections made with polarities shown in the inset. It is important here to mention that the ITO/P3HT/EV(+MoS₂ + CNT)/ITO device is actually an ECD which shows color modulation between magenta and blue under appropriate electrical bias where the representative color has been used in the schematic (inset, Figure 2b). Initially (0 V or no bias applied), the EC rectifying device is magenta (pristine color of P3HT) in color as the EV layer is transparent in this state. When 1.4 V bias across the ECD is applied such that the positive terminal is connected with the P3HT electrode as shown in the schematic (inset Figure 2b), the device changes color from magenta to blue due to the simultaneous oxidation (reduction) of P3HT (EV) to polaron (EV radical ion). This complementary redox reaction, taking place at appropriate terminals, provides the continuous supply of charge which is reflected as the current (∼0.25 mA at 1.4 V, Figure 2b) in this bias polarity state (say forward bias). The aforementioned EC rectifying device is reversible in nature due to the reversible redox activity of P3HT, and it switches its color back from blue to magenta on reversing the polarity (−1.4 V). When a negative bias is applied to an as-prepared device where the (doped-) EV layer receives a positive voltage and P3HT layer receives a negative voltage, no current flows because at this polarity (say reverse bias) the EV (P3HT) layer cannot oxidize (reduce), and hence does not allow current to flow (0 mA at −1.4 V, Figure 2b). As a consequence of the above complementary redox nature of EV and P3HT, an
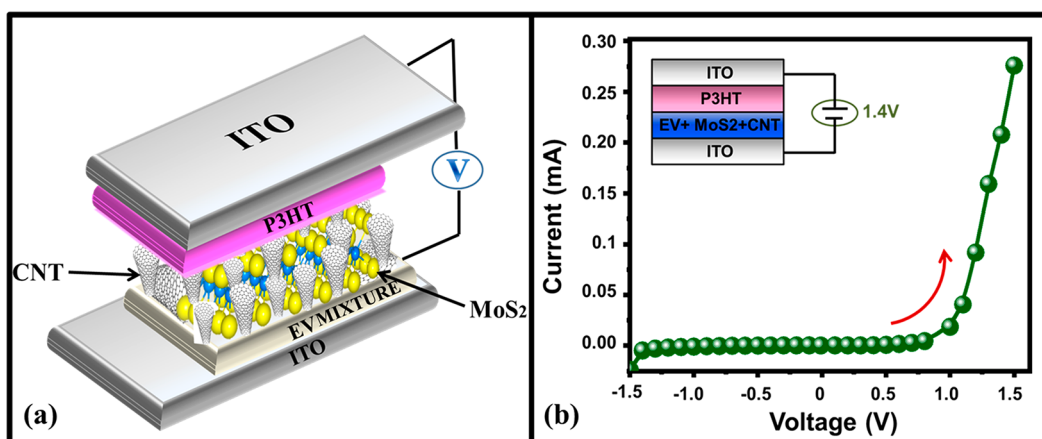
Figure 2. (a) Schematic illustration of the prepared device (along with constituent layers). (b) I−V characteristic curve at a scan rate of 100 mV/s.
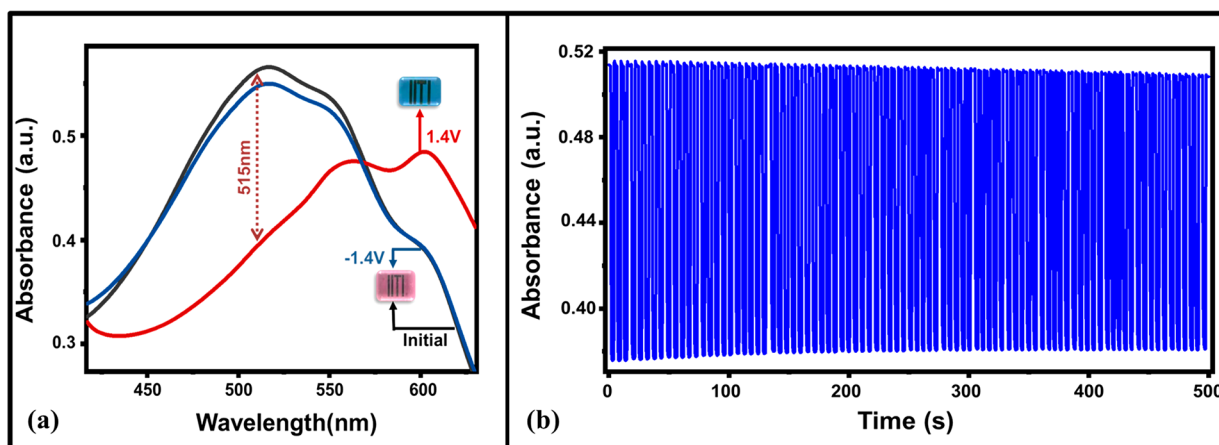
Figure 3. (a) In situ bias dependent absorption spectra of fabricated device along with photographs of the device and (b) stability of absorption cycles of device.
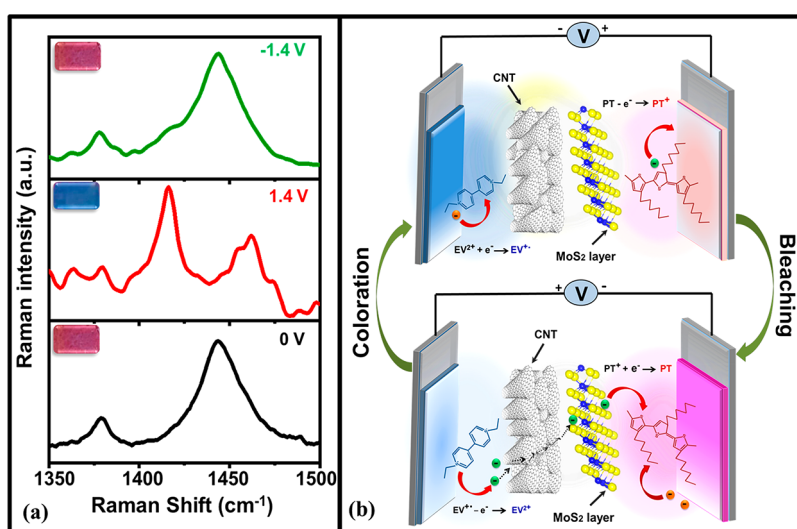
Figure 4. (a) In situ Raman spectra of the prepared solid state device under different bias conditions and (b) electron motion during the coloration and decoloration process.

asymmetric diodic I–V curve is observed which can be used for rectifying purposes, as will been discussed later.

Before exploiting the diodic I–V behavior of ECD, its color switching property has been studied using in situ UV–vis spectroscopy to see bias-induced modulation in absorbance from the device (Figure 3a) and its ability to switch multiple times (Figure 3b). Corresponding current response under the applied pulse train (±1.4 V) is shown in Figure S2 in the Supporting Information (SI). Other device parameters that quantify the performance of any ECD are switching kinetics, coloration efficiency, color contrast, and stability (cycle life) which have been estimated and presented in the SI as Figure S3a–c. The bias-dependent optical modulation from the device can be seen very clearly from the corresponding change in the absorption spectra recorded from the device (Figure 3a). The device in its as-prepared state absorbs mostly in the green region of the visible spectrum, thus appearing magenta, as can be understood from the complementary color scheme. On the other hand when forward biased, the optical response changes, and the device starts absorbing red as well as green light, thus leaving only blue to be perceived and giving the blue appearance as can be seen from the actual photograph of the device shown in

the insets. On bias reversal (reverse bias), the optical spectrum retraces the spectrum obtained from the as-prepared device which again looks magenta, and it means that the bias-induced color modulation is reversible. The color of the device in a different biasing state can also be understood through CIE diagram as shown in Figure S4 (SI) with color coordinates (u′,v′), which shift from (0.381, 0.362) to (0.198, 0.262) as the device switches its color from magenta to blue on the application of +1.4 V bias. A short film showing the color modulation and its cyclability is provided in a short film in the SI. The color switching dynamics of the device has been recorded by applying a rectangular bias (1.4 V/−1.4 V) pulse of 6 s duration (3 s each polarity) as shown in Figure S3 (SI). The device takes 0.47 s (coloration) and 0.8 s (bleaching) time to achieve an absorption change of 90% of its maximum value, which is a well-accepted definition of the switching time of a device. Coloration efficiency and color contrast (CC) of the device have also been estimated, which comes out to be 642 cm^2/C and 46%, which is one of the best performances from a P3HT based electrochromic device as shown in Figure S3 and compared in Table S1 (SI) with similar devices reported in the literature. The value of CC has been calculated using the established formula given in the SI (eq S1).
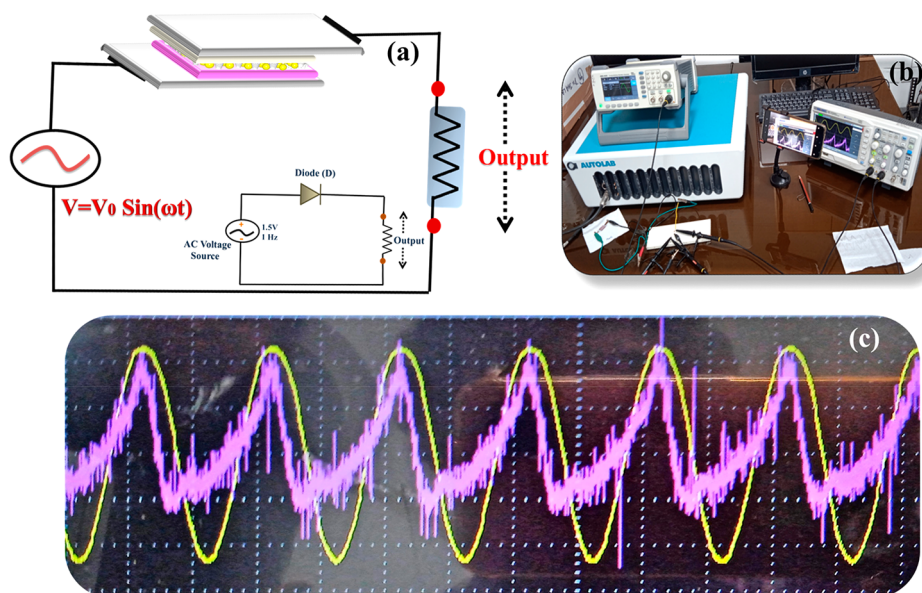
Figure 5. (a) Schematic illustration of the fabricated electrochromic rectifier with the basic circuit rectifier in the inset, (b) rectification measurement setup, and (c) input sine signal (yellow curve) and rectified signal (purple curve) using the EC diode at 1 Hz.

Stability, or cycle life, is another very important property of a device especially when one intends to use it for rectification purposes. The device has been tested to check its cyclability by observing cyclic color modulation corresponding to 515 nm wavelength by applying a constant square pulse function of (± 1.4 V, 3 s duration). The device shows a very good cycle life of at least 200 cycles (Figure 3b) without much change in the absorbance values in either of the colored states of the device. A good cycle life suggests that it is suitable for application as a rectifier as has been discussed later on.

As mentioned above, the color switching and diodic nature of the I–V curve (Figure 2b) is a consequence of bias induced redox change. To ensure that this is the mechanism for the device working, in situ Raman spectroscopy has been carried out from the device under different bias conditions. Raman spectrum of the as-fabricated device shows (0 V, black curve in Figure 4a) two peaks at 1379 and 1444 cm^{-1} which are signatures of the presence of neutral P3HT (magenta appearance). On increasing the bias to 1.4 V, the Raman spectrum changes where the above peaks shifted (red curve, Figure 4a) at 1411 cm^{-1} and ~1460[48] cm^{-1}, which indicates the formation of polaron and bipolaron, which are formed after oxidation of P3HT as expected. Transparent, blue color of polarons and bipolarons, respectively, also explains the blue appearance of the device in this forward bias condition where the EV also converts to its radical cationic state which is also blue. On bias reversal, the Raman spectrum from the device (green curve, Figure 4a) mimics the spectrum obtained from the as-prepared device (black curve, Figure 4a) confirming the reinstallation of neutral P3HT phase as can be seen as its magenta color appearance.

During the bias induced redox switching, the charge transfer in the aforementioned device is mediated by the presence of dopants which help in fast switching.[39] Initially P3HT, EV, and the dopants (MoS$_2$/CNT) are randomly distributed within a device. On the application of +ve(−ve) 1.4 V external bias to P3HT (EV) electrode, EV^{2+} starts to receive electrons (highlighted by red color) from the electrode and is reduced to (EV$^{+\cdot}$). Simultaneously P3HT loses its electrons (highlighted

by green color) to the electrode and is oxidized from its neutral state to the polaronic (ransparent) state. Since the cationic state of ethyl viologen (EV$^{+\cdot}$) has a good tendency to absorb all the visible wavelength excepts blue, the whole device starts to appear blue in color as shown in Figure 4b. On reversing the polarity, EV$^{+\cdot}$ (present from EV^{2+} reduction in the previous step) gets oxidized by transferring the excess electron to the MWCNTs/MoS$_2$ composite layered material, known for their electron holding properties, and the polaronic state of P3HT also comes back to its neutral state by accepting the necessary electron from the positive electrode, which is connected to the positive terminal of the power supply or MoS$_2$/MWCNT composite layer (Figure 4b), and the device regains its original (magenta) color. The charge stored on MoS$_2$/MWCNT layer are always accessible for faster redox activity of P3HT/EV, resulting in reducing the switching time taken to switch between the two colored states (magenta and blue) under external bias. In the absence of an electron accepting layer (MoS$_2$/MWCNT), the device will always take necessary electrons from the terminal of the power supply, which requires more time for redox activity, thus making the device slower. To see the role of MoS$_2$ and MWCNT mixing in the EV layer, control experiment have been carried out by comparing the CV curves with and without these dopants as shown in Figure S5 (SI).

For exploiting the asymmetric I–V characteristic of the device, the ECD diode has been used in a half-wave rectifier circuit (Figure 5a) where the typically used semiconductor p−n junction diode (inset, Figure 5a) has been replaced by the ECD diode. An equivalent rectifying circuit[49] was connected using the ECD diode with a load of 10Ω resistance, whereas a function generator was used to give a sinusoidal wave of 1 Hz. A digital oscilloscope was used to monitor the input (sinusoidal wave) and the output at the load resistance (rectified signal) simultaneously in an arrangement shown in Figure 5b. The half-wave rectification of a 1 Hz sine wave signal was achieved using the ECD diode as can be seen in Figure 5c, which shows the AC input voltage (1.4 V, yellow curve) and rectified signal (violet curve), in which only the positive half of the sinusoidal wave input is present and the negative half-cycle is almost absent

and appears as noise due to poor signal-to-noise filtration in the circuit. Low frequency negative voltages from sinusoidal signals can be successfully filtered using the electrochromic diode fabricated using a 2D material-doped EV/P3HT all-organic device. The layered 2D-like nanostructures of MoS_2, unique 1-dimensional electronic structure of CNT, and their tendency to trap the charges between layers and detrap under external bias lead to enhanced charge carrier mobility in one direction that eventually improves the rectification of the EC device[50,51] and can allow one to filter frequency up to 1 Hz. In the absence of these dopants, the device takes up to a few seconds to switch, thus restricting such diodes to filter only very smaller frequencies. At higher frequencies the diodic nature is not present, and thus acts as a short circuit for sinusoidal inputs. An all-organic electrochromic diode fabricated using P3HT and (MoS_2−CNT doped) EV layers switches faster than the undoped device and enables one to use these diodes for rectifying sinusoidal functions of frequencies up to 1 Hz. It is important here to mention that the color contrast of the device incorporated with MoS_2 and CNT is less than that of the device without these. Since $CNTs/MoS_2$ incorporation decreases the contrast, the amount to be incorporated in the device (to increase the coloration speed and efficiency) is limited by the desired contrast as decided by the specific application. Since color contrast is not much of a concern for rectifiers, one can use the maximum amount of these dopants to achieve the fastest possible rectifier.

4. CONCLUSION

An asymmetric I−V characteristic, similar to diodic behavior, observed from a solid state electrochromic diode device can be used for rectification purposes to filter a sinusoidal voltage of frequency up to 1 Hz or less. A solid state electrochromic diode, fabricated using an organic electrochromic conducting polymer P3HT and EV (doped with MoS_2/MWCNTs composites) shows reversible color modulation between magenta and blue colors when a bias of ± 1.4 V is applied. In situ bias-dependent UV−vis spectroscopy reveals the aforementioned color modulation with switching time (0.47 s/0.8 s), 46% color contrast with excellent coloration efficiency of 642 cm^2/C, and a good cycle life/stability of the electrochromic diode. In situ Raman spectroscopy establishes that the color modulation is caused by the bias induced redox switching as a consequence of dynamic doping in P3HT. It has been observed that doping of MWCNTs and MoS_2 makes the device switch faster as compared to the basic EV/P3HT device making it suitable for rectification of AC voltages up to 1 Hz. Its charge holding property between conducting polymer layers (P3HT and EV) enhanced the forward-bias current and rectification ratio. This property of the MoS_2/MWCNTs composite reduces the dependency of the redox activity on the power supply and switching time of the device between the two colored states (magenta and blue). To demonstrate the use of the EC device in rectifier circuits, its frequency response also has been evaluated, which indicates its low frequency rectifying nature with an input oscillating voltage of ± 1.4 V. The device fabricated by the doping of 2D layered material or charge holding materials between the EC-conducting polymer layer can provide reversibility, electrochromism, and rectifying behaviors in a single solid state device and thus opens up new possibilities to fabricate other organic electrochromic and rectifying devices that operate on a simple oxidation/reduction principle.

■ ASSOCIATED CONTENT

ⓈⒾ Supporting Information

The Supporting Information is available free of charge at https://pubs.acs.org/doi/10.1021/acsmaterialsau.1c00064.

Additional data to test device performance, characterization images of electrodes, device performance comparison, CIE diagram of device, and additional CV curves (PDF)

Video showing bias induced color change and cyclic response (MP4)

■ AUTHOR INFORMATION

Corresponding Author

Rajesh Kumar − *Materials and Device Laboratory, Department of Physics, Centre for Advanced Electronics, Centre for Rural Development and Technology, and Centre for Indian Scientific Knowledge Systems, Indian Institute of Technology Indore, Simrol 453552, India;* Ⓞ orcid.org/0000-0001-7977-986X; Email: rajeshkumar@iiti.ac.in

Authors

Suchita Kandpal − *Materials and Device Laboratory, Department of Physics, Indian Institute of Technology Indore, Simrol 453552, India*

Tanushree Ghosh − *Materials and Device Laboratory, Department of Physics, Indian Institute of Technology Indore, Simrol 453552, India;* Ⓞ orcid.org/0000-0001-7160-685X

Chanchal Rani − *Materials and Device Laboratory, Department of Physics, Indian Institute of Technology Indore, Simrol 453552, India*

Manushree Tanwar − *Materials and Device Laboratory, Department of Physics, Indian Institute of Technology Indore, Simrol 453552, India;* Ⓞ orcid.org/0000-0002-7589-0496

Meenu Sharma − *Department of Physics, Guru Jambheshwar University of Science & Technology, Hisar 125001, India*

Sonam Rani − *Department of Physics, Guru Jambheshwar University of Science & Technology, Hisar 125001, India*

Devesh K. Pathak − *Materials and Device Laboratory, Department of Physics, Indian Institute of Technology Indore, Simrol 453552, India;* Ⓞ orcid.org/0000-0002-2367-787X

Ravi Bhatia − *Department of Physics, Guru Jambheshwar University of Science & Technology, Hisar 125001, India*

I. Sameera − *Department of Physics, Guru Jambheshwar University of Science & Technology, Hisar 125001, India*

Jesumony Jayabalan − *Homi Bhabha National Institute, Mumbai 400094, India*

Complete contact information is available at:
https://pubs.acs.org/10.1021/acsmaterialsau.1c00064

Notes

The authors declare no competing financial interest.

■ ACKNOWLEDGMENTS

■ REFERENCES

(1) Chua, M. H.; Tang, T.; Ong, K. H.; Neo, W. T.; Xu, J. W. Introduction to Electrochromism. In *Electrochromic Smart Materials: Fabrication and Application*, Xu, J. W.; Chua, M. H.; Shah, K. W., Eds.; Royal Society of Chemistry; 2019; Chapter 1, pp 1–21. DOI: 10.1039/9781788016667-00001.

(2) Kumar, R.; Pathak, D. K.; Chaudhary, A. Current Status of Some Electrochromic Materials and Devices: A Brief Review. *J. Phys. D: Appl. Phys.* 2021, *54*, 503002.

(3) Mishra, S.; Lambora, S.; Yogi, P.; Sagdeo, P. R.; Kumar, R. Organic Nanostructures on Inorganic Ones: An Efficient Electrochromic Display by Design. *ACS Appl. Nano Mater.* 2018, *1* (7), 3715–3723.

(4) Pathak, D. K.; Chaudhary, A.; Tanwar, M.; Goutam, U. K.; Kumar, R. Nano-Cobalt Oxide/Viologen Hybrid Solid State Device: Electrochromism beyond Chemical Cell. *Appl. Phys. Lett.* 2020, *116* (14), 141901.

(5) Chaudhary, A.; Pathak, D. K.; Ghosh, T.; Kandpal, S.; Tanwar, M.; Rani, C.; Kumar, R. Prussian Blue-Cobalt Oxide Double Layer for Efficient All-Inorganic Multicolor Electrochromic Device. *ACS Appl. Electron. Mater.* 2020, *2* (6), 1768–1773.

(6) Mjejri, I.; Doherty, C. M.; Rubio-Martinez, M.; Drisko, G. L.; Rougier, A. Double-Sided Electrochromic Device Based on Metal–Organic Frameworks. *ACS Appl. Mater. Interfaces* 2017, *9* (46), 39930–39934.

(7) Barawi, M.; Veramonti, G.; Epifani, M.; Giannuzzi, R.; Sibillano, T.; Giannini, C.; Rougier, A.; Manca, M. A Dual Band Electrochromic Device Switchable across Four Distinct Optical Modes. *J. Mater. Chem. A* 2018, *6* (22), 10201–10205.

(8) Yang, P.; Sun, P.; Mai, W. Electrochromic Energy Storage Devices. *Mater. Today* 2016, *19* (7), 394–402.

(9) Xia, X.; Zhang, Y.; Chao, D.; Guan, C.; Zhang, Y.; Li, L.; Ge, X.; Mínguez Bacho, I.; Tu, J.; Jin Fan, H. Solution Synthesis of Metal Oxides for Electrochemical Energy Storage Applications. *Nanoscale* 2014, *6* (10), 5008–5048.

(10) Laforgue, A.; Simon, P.; Sarrazin, C.; Fauvarque, J.-F. Polythiophene-Based Supercapacitors. *J. Power Sources* 1999, *80* (1), 142–148.

(11) Chen, S.; Xing, W.; Duan, J.; Hu, X.; Qiao, S. Z. Nanostructured Morphology Control for Efficient Supercapacitor Electrodes. *Journal of Materials Chemistry A* 2013, *1* (9), 2941–2954.

(12) Chaudhary, A.; Pathak, D. K.; Tanwar, M.; Sagdeo, P. R.; Kumar, R. Prussian Blue-Viologen Inorganic–Organic Hybrid Blend for Improved Electrochromic Performance. *ACS Applied Electronic Materials* 2019, *1*, 892.

(13) Pathak, D. K.; Chaudhary, A.; Tanwar, M.; Goutam, U. K.; Mondal, P.; Kumar, R. Nickel Cobalt Oxide Nanoneedles for Electrochromic Glucose Sensors. *ACS Appl. Nano Mater.* 2021, *4* (2), 2143–2152.

(14) Yan, N.; Song, J.; Wang, F.; Kan, L.; Song, J.; Wang, W.; Ma, W.; Zhang, W.; He, G. Pyrenoviologen-Based Fluorescent Sensor for Detection of Picric Acid in Aqueous Solution. *Chin. Chem. Lett.* 2019, *30* (11), 1984–1988.

(15) Mortimer, R. J.; Dyer, A. L.; Reynolds, J. R. Electrochromic Organic and Polymeric Materials for Display Applications. *Displays* 2006, *27* (1), 2–18.

(16) Barile, C. J.; Slotcavage, D. J.; McGehee, M. D. Polymer–Nanoparticle Electrochromic Materials That Selectively Modulate

Visible and Near-Infrared Light. *Chem. Mater.* 2016, *28* (5), 1439–1445.

(17) Chaudhary, A.; Poddar, M.; Pathak, D. K.; Misra, R.; Kumar, R. Electron Donor Ferrocenyl Phenothiazine: Counter Ion for Improving All-Organic Electrochromism. *ACS Appl. Electron. Mater.* 2020, *2* (9), 2994–3000.

(18) Chaudhary, A.; Sivakumar, G.; Pathak, D. K.; Tanwar, M.; Misra, R.; Kumar, R. Pentafluorophenyl Substituted Fulleropyrrolidine: A Molecule Enabling the Most Efficient Flexible Electrochromic Device with Fast Switching. *Journal of Materials Chemistry C* 2021, *9* (10), 3462–3469.

(19) Chen, M. Printed Electrochemical Devices Using Conducting Polymers as Active Materials on Flexible Substrates. *Proc. IEEE* 2005, *93* (7), 1339–1347.

(20) Chaudhary, A.; Pathak, D. K.; Tanwar, M.; Yogi, P.; Sagdeo, P. R.; Kumar, R. Polythiophene–PCBM-Based All-Organic Electrochromic Device: Fast and Flexible. *ACS Applied Electronic Materials* 2019, *1*, 58.

(21) Cai, G.; Tu, J.; Zhou, D.; Li, L.; Zhang, J.; Wang, X.; Gu, C. Constructed TiO2/NiO Core/Shell Nanorod Array for Efficient Electrochromic Application. *J. Phys. Chem. C* 2014, *118* (13), 6690–6696.

(22) da Silva, A. J. C.; Ribeiro Nogueira, F. A.; Tonholo, J.; Ribeiro, A. S. Dual-Type Electrochromic Device Based on Polypyrrole and Polythiophene Derivatives. *Sol. Energy Mater. Sol. Cells* 2011, *95* (8), 2255–2259.

(23) Penin, N.; Rougier, A.; Laffont, L.; Poizot, P.; Tarascon, J.-M. Improved Cyclability by Tungsten Addition in Electrochromic NiO Thin Films. *Sol. Energy Mater. Sol. Cells* 2006, *90* (4), 422–433.

(24) Maruyama, T.; Arai, S. Electrochromic Properties of Cobalt Oxide Thin Films Prepared by Chemical Vapor Deposition. *J. Electrochem. Soc.* 1996, *143* (4), 1383.

(25) Kim, S. Y.; Yun, T. Y.; Yu, K. S.; Moon, H. C. Reliable, High-Performance Electrochromic Supercapacitors Based on Metal-Doped Nickel Oxide. *ACS Appl. Mater. Interfaces* 2020, *12* (46), 51978–51986.

(26) Chaudhary, A.; Ghosh, T.; Pathak, D. K.; Kandpal, S.; Tanwar, M.; Rani, C.; Kumar, R. Prussian Blue-Based Inorganic Flexible Electrochromism Glucose Sensor. *IET Nanodielectrics* 2021, *4*, 165.

(27) Chaudhary, A.; Pathak, D. K.; Kandpal, S.; Ghosh, T.; Tanwar, M.; Kumar, R. Raw Hibiscus Extract as Redox Active Biomaterial for Novel Herbal Electrochromic Device. *Sol. Energy Mater. Sol. Cells* 2020, *215*, 110588.

(28) Mitchell, R. H.; Brkic, Z.; Sauro, V. A.; Berg, D. J. A Photochromic, Electrochromic, Thermochromic Ru Complexed Benzannulene: An Organometallic Example of the Dimethyldihydropyrene–Metacyclophanediene Valence Isomerization. *J. Am. Chem. Soc.* 2003, *125* (25), 7581–7585.

(29) Moon, H. C.; Kim, C.-H.; Lodge, T. P.; Frisbie, C. D. Multicolored, Low-Power, Flexible Electrochromic Devices Based on Ion Gels. *ACS Appl. Mater. Interfaces* 2016, *8* (9), 6252–6260.

(30) Moon, H. C.; Lodge, T. P.; Frisbie, C. D. Solution Processable, Electrochromic Ion Gels for Sub-1 V, Flexible Displays on Plastic. *Chem. Mater.* 2015, *27* (4), 1420–1425.

(31) Chakraborty, C.; Pandey, R. K.; Rana, U.; Kanao, M.; Moriyama, S.; Higuchi, M. Geometrically Isomeric Pt(II)/Fe(II)-Based Heterometallo-Supramolecular Polymers with Organometallic Ligands for Electrochromism and the Electrochemical Switching of Raman Scattering. *J. Mater. Chem. C* 2016, *4* (40), 9428–9437.

(32) Pathak, D. K.; Chaudhary, A.; Tanwar, M.; Goutam, U. K.; Pfnür, H.; Kumar, R. Chronopotentiometric Deposition of Nanocobalt Oxide for Electrochromic Auxiliary Active Electrode Application. *physica status solidi (a)* 2020, *217* (19), 2000173.

(33) Sheng, K.; Bai, H.; Sun, Y.; Li, C.; Shi, G. Layer-by-Layer Assembly of Graphene/Polyaniline Multilayer Films and Their Application for Electrochromic Devices. *Polymer* 2011, *52* (24), 5567–5572.

(34) Kim, M.; Ki Kim, Y.; Kim, J.; Cho, S.; Lee, G.; Jang, J. Fabrication of a Polyaniline/MoS 2 Nanocomposite Using Self-Stabilized

Dispersion Polymerization for Supercapacitors with High Energy Density. *RSC Adv.* **2016**, *6* (33), 27460−27465.

(35) Mishra, S.; Pandey, H.; Yogi, P.; Saxena, S. K.; Roy, S.; Sagdeo, P. R.; Kumar, R. In-Situ Spectroscopic Studies of Viologen Based Electrochromic Device. *Opt. Mater.* **2017**, *66*, 65−71.

(36) Mishra, S.; Pandey, H.; Yogi, P.; Saxena, S. K.; Roy, S.; Sagdeo, P. R.; Kumar, R. Live Spectroscopy to Observe Electrochromism in Viologen Based Solid State Device. *Solid State Commun.* **2017**, *261*, 17−20.

(37) Chang, X.; Sun, S.; Dong, L.; Hu, X.; Yin, Y. Tungsten Oxide Nanowires Grown on Graphene Oxide Sheets as High-Performance Electrochromic Material. *Electrochim. Acta* **2014**, *129*, 40−46.

(38) Kandpal, S.; Ghosh, T.; Sharma, M.; Pathak, D. K.; Tanwar, M.; Rani, C.; Bhatia, R.; Sameera, I.; Chaudhary, A.; Kumar, R. Multi-Walled Carbon Nanotubes Doping for Fast and Efficient Hybrid Solid State Electrochromic Device. *Appl. Phys. Lett.* **2021**, *118* (15), 153301.

(39) Mishra, S.; Kumar, R. Graphene Nanoflakes: Foundation for Improving Solid State Electrochemistry Based Electrochromic Devices. *Sol. Energy Mater. Sol. Cells* **2019**, *200*, 110041.

(40) Suarez, D.; Steven, E.; Laukhina, E.; Gomez, A.; Crespi, A.; Mestres, N.; Rovira, C.; Choi, E. S.; Veciana, J. 2D Organic Molecular Metallic Soft Material Derived from BEDO-TTF with Electrochromic and Rectifying Properties. *npj Flex Electron* **2018**, *2* (1), 1−7.

(41) Deokar, G.; Vancsó, P.; Arenal, R.; Ravaux, F.; Casanova-Cháfer, J.; Llobet, E.; Makarova, A.; Vyalikh, D.; Struzzi, C.; Lambin, P.; Jouiad, M.; Colomer, J.-F. MoS2−Carbon Nanotube Hybrid Material Growth and Gas Sensing. *Advanced Materials Interfaces* **2017**, *4* (24), 1700801.

(42) Li, H.; Zhang, Q.; Yap, C. C. R.; Tay, B. K.; Edwin, T. H. T.; Olivier, A.; Baillargeat, D. From Bulk to Monolayer MoS2: Evolution of Raman Scattering. *Adv. Funct. Mater.* **2012**, *22* (7), 1385−1390.

(43) Lee, C.; Yan, H.; Brus, L. E.; Heinz, T. F.; Hone, J.; Ryu, S. Anomalous Lattice Vibrations of Single- and Few-Layer MoS2. *ACS Nano* **2010**, *4* (5), 2695−2700.

(44) Kandpal, S.; Ghosh, T.; Rani, C.; Rani, S.; Pathak, D. K.; Tanwar, M.; Bhatia, R.; Sameera, I.; Kumar, R. MoS2 Nano-Flower Incorporation for Improving Organic-Organic Solid State Electrochromic Device Performance. *Sol. Energy Mater. Sol. Cells* **2022**, *236*, 111502.

(45) Sharma, M.; Rani, S.; Pathak, D. K.; Bhatia, R.; Kumar, R.; Sameera, I. Manifestation of Anharmonicities in Terms of Phonon Modes' Energy and Lifetime in Multiwall Carbon Nanotubes. *Carbon* **2021**, *171*, 568−574.

(46) Bhatia, R.; Prasad, V.; Menon, R. Characterization, Electrical Percolation and Magnetization Studies of Polystyrene/Multiwall Carbon Nanotube Composite Films. *Materials Science and Engineering: B* **2010**, *175* (3), 189−194.

(47) Windom, B. C.; Sawyer, W. G.; Hahn, D. W. A Raman Spectroscopic Study of MoS2 and MoO3: Applications to Tribological Systems. *Tribol. Lett.* **2011**, *42* (3), 301−310.

(48) Yamamoto, J.; Furukawa, Y. Raman Characterization and Electrical Properties of Poly(3-Hexylthiophene) Doped Electrochemically in an Ionic Liquid-Gated Transistor Geometry. *Org. Electron.* **2016**, *28*, 82−87.

(49) Heljo, P. S.; Li, M.; Lilja, K. E.; Majumdar, H. S.; Lupo, D. Printed Half-Wave and Full-Wave Rectifier Circuits Based on Organic Diodes. *IEEE Trans. Electron Devices* **2013**, *60* (2), 870−874.

(50) Mallikarjuna, K.; Shinde, M. A.; Kim, H. Electrochromic Smart Windows Using 2D-MoS2 Nanostructures Protected Silver Nanowire Based Flexible Transparent Electrodes. *Materials Science in Semiconductor Processing* **2020**, *117*, 105176.

(51) Mahmood, Q.; Park, S. K.; Kwon, K. D.; Chang, S.-J.; Hong, J.-Y.; Shen, G.; Jung, Y. M.; Park, T. J.; Khang, S. W.; Kim, W. S.; Kong, J.; Park, H. S. Transition from Diffusion-Controlled Intercalation into Extrinsically Pseudocapacitive Charge Storage of MoS2 by Nanoscale Heterostructuring. *Adv. Energy Mater.* **2016**, *6* (1), 1501115.